Assessing the ability of interactive pipe liners to withstand host-pipe failure*

B. B. Crunkhorn, J. T. Whiter, A. Ham, M. Mulheron and P. A. Smith

ABSTRACT

This paper presents an investigation into the behaviour of a number of pipe liner materials, with the specific aim of determining their ability to remain intact during failure of the cast iron host main. Three different liner systems have been evaluated along with an unlined control. One of the liners (epoxy resin lining) is a non-structural technique, whereas the other two (Subcoil and a new development) are semi-structural (or interactive) liners.

Metallographic analysis and tensile tests were carried out on small samples cut from the cast iron host pipe in order to characterise the basic properties of the cast iron. Metallography revealed a microstructure typical of a grey cast iron, consisting of acicular graphite flakes with some rosettes; etching with 2% Nital acid etch revealed the presence of pearlite. Tensile tests on small samples cut from the pipes indicated significant non-linearity in the stress-strain response. Lined cast iron pipes were tested to failure in four-point bending. A circumferential notch was machined into the wall of some of the pipes, in order to simulate the reduction in host-pipe strength due to corrosion. In addition some tests were carried out under applied internal water pressure, to determine if this had any effect on liner behaviour. Both interactive liners survived host-pipe failure, whilst, as expected, the non-structural liner did not. A simple method was developed which enabled the bending moment curvature relationship in a bend test to be modelled from tensile data; this model gave satisfactory agreement with the experimental data.

Key words | cast iron, pipe liner, renovation, semi-structural, water main

B. B. Crunkhorn (corresponding author)
School of Engineering,
University of Surrey,
Guildford, Surrey GU2 7XH,
UK
and
Thames Water,
Environment and Technology,
Spencer House,
Manor Farm Road,
Reading, Berkshire RG2 0JN,
UK
E-mail: *Ben.crunkhorn@thameswater.co.uk*

M. Mulheron
P. A. Smith
School of Engineering,
University of Surrey,
Guildford, Surrey GU2 7XH,
UK

J. T. Whiter
A. Ham
Thames Water,
Environment and Technology,
Spencer House,
Manor Farm Road,
Reading, Berkshire RG2 0JN,
UK

INTRODUCTION

There are over 295,000 km of water mains in England and Wales, the majority of which are made from cast iron. In some areas, such as inner London, they may be up to 150 years old. It is likely that some sections of the network are approaching the end of their useful service life. This is due to degradation of the water distribution network which is believed to be a time dependent process. Factors such as internal and external corrosion, repeated loading by traffic and changes in temperature are all thought to influence the lifetime of a pipe. For a given service loading, the more of these factors that act on a water main and the greater their severity, the shorter is the expected service life of the pipe.

As water networks reach the end of their useful life it is important for the industry to identify appropriate interventions, including suitable rehabilitation or renovation techniques. There are many such techniques available, which vary in respect of, amongst other factors, the material used, the degree of structural strength the liner possesses and the method of installation. In order to differentiate between the many rehabilitation techniques it is common to characterise them as being non-, semi- or fully structural. It is the semi-structural (or interactive) liners that are of interest in this work. The term semi-structural indicates that the liner can withstand some of

*The opinions expressed in this work and the conclusions reached are those of the authors and are not necessarily endorsed by Thames Water.

the expected service loads, but not all. This is in contrast with non-structural liners, where all loads are borne by the host main, and fully structural liners, where the liner is considered to be capable of withstanding all the expected loads for the duration of the design life.

At present, interactive liner systems (BS EN 13689: 2002) tend to be used under conditions of minimal load bearing requirement; that is, the load borne by the liner under transient conditions, such as soil loading, or more dynamic conditions, such as those associated with pipe fracture, is assumed to be negligible. In the future, however, the use of interactive liners may increase for two main reasons. Firstly, the installation and operation of these liners are becoming cheaper and so are likely to become more cost effective. Secondly, as the age of the pipe network increases the use of liners to prolong asset life, and control leakage, is likely to become more widespread. However, in order to justify an increased use of such liners, an improved understanding of their likely behaviour in service is required.

The analysis of interactive liners under service conditions must consider a variety of mechanical and chemical factors and their interactions. Some research has been conducted on some interactive liner systems in order to determine their structural properties and performance limits (Boot *et al.* 1996; Boot and Welch 1996). There is also published work (Gumbel 1997; Boot and Toropova 1999) regarding the response of interactive liners to different service conditions. These latter studies have focused on the behaviour under 'hole-spanning' and 'gap-bridging' conditions and have used a combination of mechanical test data and finite element analysis to predict the performance of liners under a given loading regime. However, there has been little systematic investigation of the available interactive liner techniques, both individually and as a generic group.

This paper describes mechanical testing carried out on cast iron pipes with three different liners: (i) an epoxy resin lining, ELC 257/91; (ii) Subcoil, a thin walled polyethylene liner; and (iii) a developmental polymeric lining system. The last two are semi-structural liners, whereas the first is a non-structural system. Epoxy resin lining is the least expensive of the three liners considered. The interactive liners are both more expensive than the epoxy system, but offer greater long-term benefits, particularly regarding potential reductions in leakage against which increased costs may be offset. The main aim of the initial stage of the work was to examine the performance of the three liners under a severe loading condition, that is, catastrophic fracture of the host pipe.

The majority of water mains in the UK are in the diameter range 4–8 inches. An experimental investigation considering the case of a lined 4 inch cast iron pipe was therefore carried out. Such mains typically fail under flexurally (bending) induced circumferential fracture (UKWIR 1999), and hence this was the failure condition studied in this work. The effect of water pressure on both the failure strength of the cast iron and the behaviour of the liner during failure was also considered, as was the likely effect of corrosion, which was simulated by the introduction of a circumferential notch.

The structure of the present paper is as follows. The next section comprises a description of the experimental work. The results from the microstructural and mechanical characterisation of the cast-iron pipes are then presented. The non-linear behaviour of the cast iron is sufficiently pronounced that an analytical model is required to interpret the bend test data; the moment-curvature relationship is determined and a method of estimating the maximum stress in the host-pipe at fracture is suggested. The penultimate section considers the experimental behaviour of the lined cast iron pipes in bending, with reference to these model calculations; finally, the main conclusions from the work are presented.

EXPERIMENTAL WORK

Materials

Cast iron pipes were manufactured specifically for this work, rather than sourcing them from pipes in service in the ground. There were two reasons for this. Firstly, as-manufactured pipe is likely to have more repeatable failure strengths than pipes taken from the ground, which may be of differing age and manufacturing method, as well as different states of repair. Secondly, new pipe was easier

to acquire in the quantities required for these studies. The pipes themselves were manufactured using a horizontal sand casting process and were supplied in flanged 1.8 m lengths. In general new pipe is expected to have a higher failure strength than pipe taken from the ground and this will represent a severe test of the liners. Some of the pipe samples had a circumferential notch (nominal depth, $a = 3$ mm and root radius, $\rho = 1$ mm) machined into the wall at the mid-span, using a lathe, to simulate the effect of corrosion. The actual depth of the machined notch was measured from the fracture surface of the failed pipe.

The notation to distinguish the individual pipe samples was as follows. The first two letters indicate the pipe-liner system used: UL for the unlined control, EL for epoxy resin lining, SC for Subcoil and ND for the new development. Epoxy resin lining is a spray lining technique, which applies a layer of the resin approximately 1 mm thick to the host-pipe. Subcoil is winched into the main in a folded 'C' shape and subsequently reverted using mains water pressure. Subsequent letters are 'UN' (for un-notched pipes) or 'N' (for notched pipes) followed by a number that indicates the individual specimen in a particular test series. A 'W' at the end indicates that the test was carried out on a pipe pressurised with water.

Metallographic analysis

A number of small samples were taken from sections of pipe, in both the longitudinal and transverse directions. These samples were mounted in standard Bakelite mounts and subsequently polished to a 1 μm finish; some samples were additionally etched using 2% Nital acid etch. Samples were then examined using light microscopy and images were recorded using an attached digital camera with a resolution of 1260 × 960 pixels (1.2 Megapixels).

Tensile testing

Tensile test pieces were machined from the walls of three of the pipes. These 'dog-bone' samples had dimensions 150 mm × 20 mm × 5 mm with a central gauge length that was 80 mm × 10 mm × 5 mm. The samples were loaded to failure using an Instron 5500 tensile testing machine, under displacement control, at a nominal extension rate of 0.1 mm min^{-1}. The strain was measured using the average value from two longitudinally oriented strain gauges, one located on either side of the specimen.

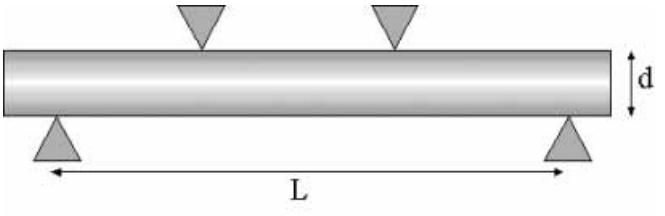

Figure 1 | The four-point loading geometry (in this work $L = 1.2$ m, and the central gauge length $L/2$ is 0.6 m).

Flexural testing

The various pipe configurations were loaded to failure in four-point bending under displacement control, at a rate of 1 mm min^{-1}, using an Instron 8800 servo-hydraulic testing machine; see Figure 1 for a schematic representation of the test geometry. Mild steel cradles were manufactured which enabled the pipes to be loaded to failure without generating significant stress levels at the loading points. Four-point bending was chosen since the maximum bending moment is experienced over a significant volume of the sample. In comparison with a three-point bending arrangement this increases the chances of a representative critical defect being present in the test volume.

In some cases water pressure was applied inside the liner, in order to simulate service conditions more realistically. The pipes were sealed by applying end flanges to either end of the pipe after first terminating the end of the liner in the standard manner for the technique. Water pressure was regulated by means of a pressure release valve, such that a constant pressure of 10 bar was achieved prior to the start of each test. The pressure was monitored during the tests using a pressure sensitive actuator placed within one of the flanges. During each test the displacement of the machine crosshead and the applied load were measured. In some tests the surface strain at the crown and invert of the specimen was also measured using strain

Figure 2 | Pipe section under test showing load application through a spreader beam.

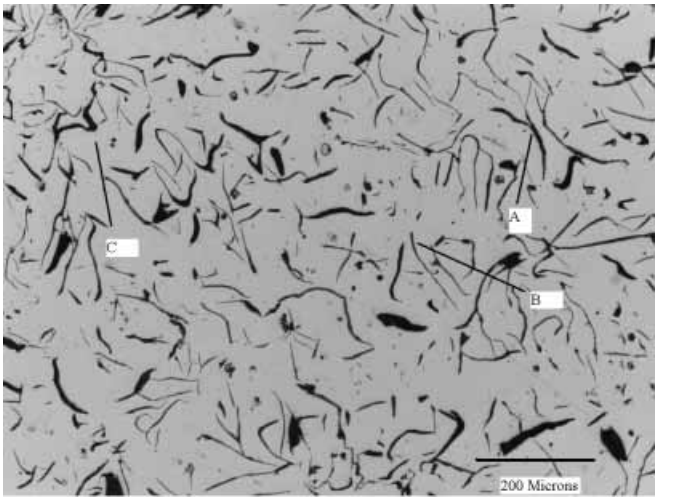

Figure 3 | Microstructure of the un-etched cast iron.

gauges. Figure 2 shows the general arrangement of a pipe specimen under test.

The behaviour of the various liners was observed visually during the tests and following failure. The interactive liners were considered to have survived the test if no hole was found to be present in the liner following host-pipe failure. This was determined by visual inspection for tests without applied water pressure; in the pressurised tests the presence of a water leak was taken to indicate perforation of the liner.

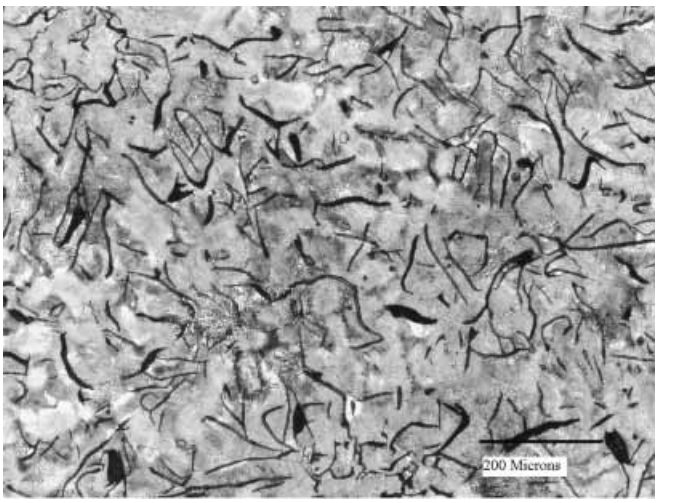

Figure 4 | Low magnification photomicrograph of an etched section of pipe.

MICROSTRUCTURAL ANALYSIS AND STRESS-STRAIN BEHAVIOUR OF THE CAST IRON

Metallographic analysis

Microstructural analysis carried out on the pipes revealed typical features for a horizontally cast grey cast iron. Figure 3 shows a typical area of the un-etched microstucture. Figure 4 shows the same area as Figure 3, but the microstructure has been etched using 2% Nital.

From Figure 3 it can be seen that graphite flakes are present in three different morphologies, namely acicular (A), scythe shaped (B) and rosette (C). These different microstructures are thought to result from differing cooling rates being experienced across the pipe section. From Figure 4 it is apparent that the microstructure is predominantly pearlitic. This is confirmed in Figure 5, which shows a pearlitic region at higher magnification.

Tensile testing

Figure 6 shows typical stress-strain curves for each of the three cast iron pipes tested. Four samples were tested from

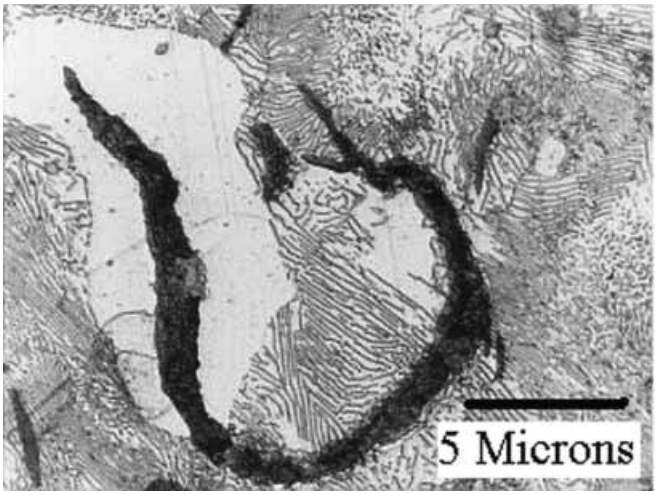

Figure 5 | Photomicrograph depicting regions of pearlite within the etched microstructure.

each of three pipes; the notation in Figure 6 cross-references the corresponding pipe test. Samples from a given pipe show consistent behaviour although there is some variability in samples from different pipes. Such variation seems reasonable, bearing in mind that the pipes were manufactured in two distinct batches (ULN1 was from one batch while ULUN3W and ULUN5W were from the other batch) and that there is variability in the material response, which will depend upon the exact composition and processing.

Figures 7 and 8 enable the measured tensile properties of the material used in this work to be compared with published data for a similar material. Figure 7 shows the stress-strain behaviour, while Figure 8 shows the secant Young's modulus as a function of applied strain. The figures show clearly the non-linear behaviour of the material used for the present work. At low strains the behaviour appears similar to published data, but it diverges at higher strains.

Given the marked non-linearity, there are a number of methods that can be used to obtain a measure of the Young's modulus. The approach adopted here was to fit a fifth order polynomial to the stress-strain curve and then determine analytically the value of the slope at the origin. The resulting values from the 12 tensile samples are shown in Table 1. While the data from each pipe are consistent, it can be seen that the material from pipe ULN1W has a lower stiffness (as was also apparent from the stress/strain data).

Material non-linearity will also influence the response of the pipes loaded in flexure. Hence in the next section we consider the modifications necessary to simple elastic

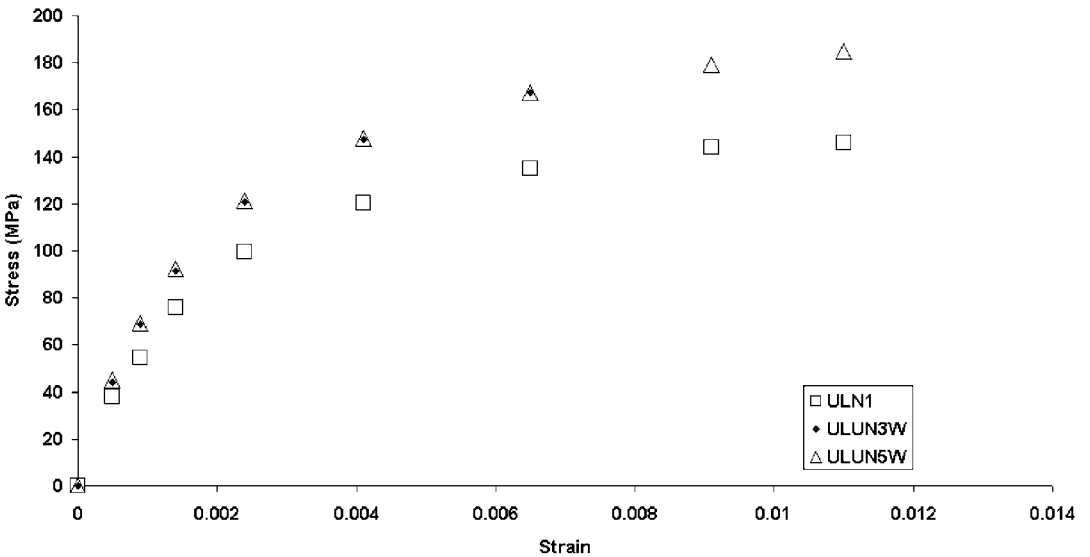

Figure 6 | Plot of stress against strain for the 12 test pieces.

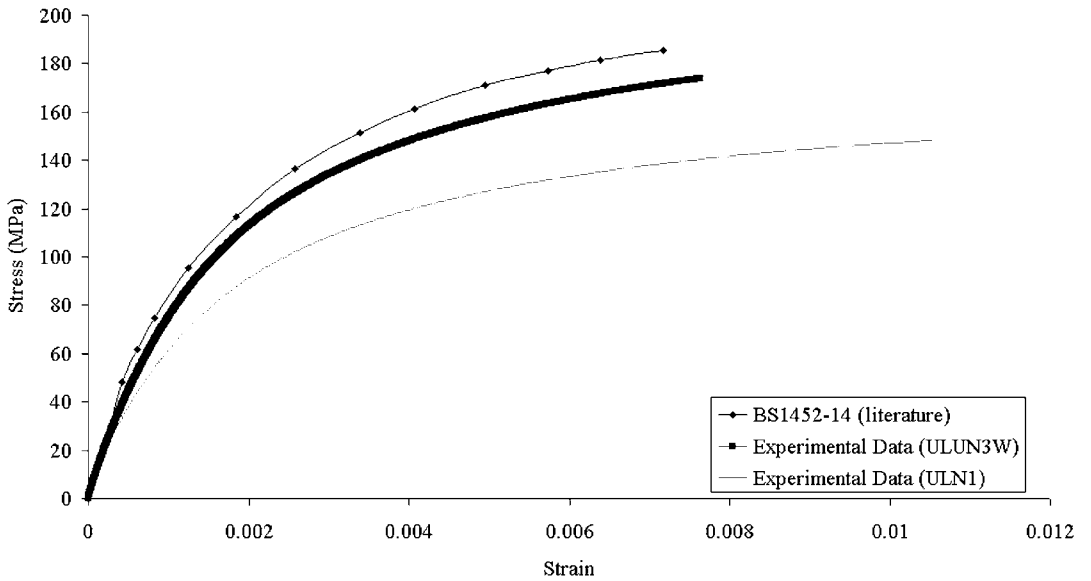

Figure 7 | Stress/strain plots for three different cast iron materials, a literature benchmark (Angus 1976) and two sets of experimental data from the present work.

bending theory that will enable this to be taken into account.

THEORETICAL BACKGROUND

Elastic analysis

According to simple elastic bending theory,

$$\frac{M}{I} = \frac{\sigma}{y} = \frac{E}{R} \tag{1}$$

In Equation (1), σ denotes the stress in the beam at distance y from the neutral axis of the section, M is the applied bending moment, I is the second moment of area of the section about its neutral axis, R is the radius of curvature of the deformed beam and E is the Young's modulus of the material.

In earlier reports of part of this study (Crunkhorn *et al.* 2001), Equation (1) was used to analyse the test data. However, as seen in the previous section, the tensile behaviour of the cast iron is significantly non-linear (Figure 8) and hence non-linear methods have to be used to analyse the data more fully, as developed below. The aim of the analysis is twofold, to determine the moment-curvature relationship and to estimate the stress in the cast iron when the pipes fracture.

Predicting the moment-curvature relationship of a beam of non-linear material

For the four-point bending geometry (Figure 1) used in this work, the applied bending moment may be found using Equation (2).

$$M = \frac{FL}{8} \tag{2}$$

where, F is the applied force and L is the length of the specimen.

Assuming that plane sections remain plane, the strain at distance y from the neutral axis of the pipe is related to the curvature of the pipe, $\varkappa$, by,

$$\varepsilon = y\varkappa \tag{3}$$

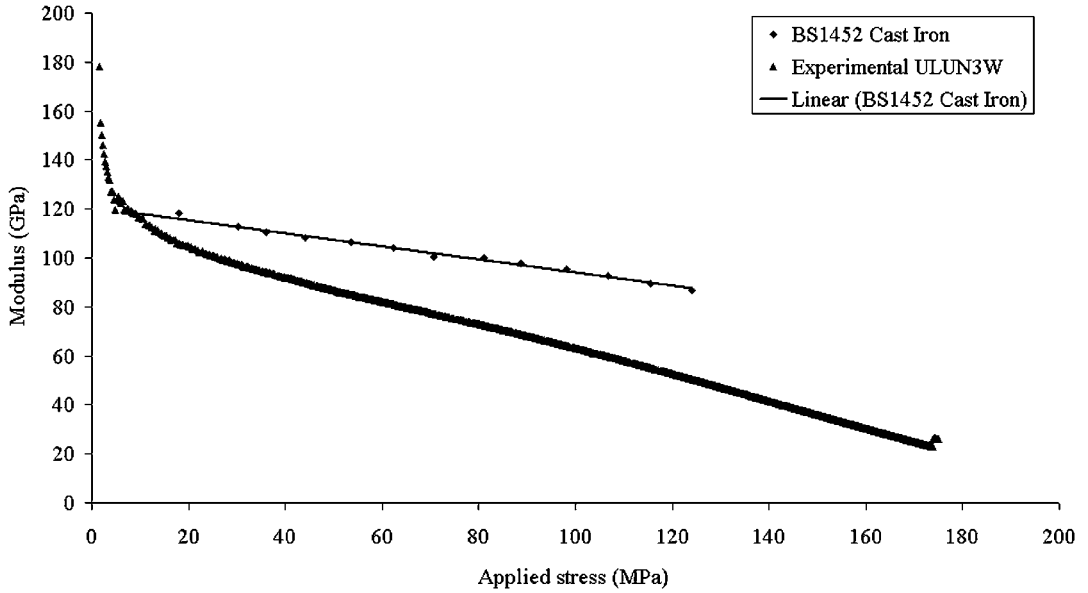

Figure 8 | Variation of modulus with applied stress, showing both experimental and literature data (Angus 1976).

Table 1 | Young's modulus values obtained from the tensile specimens; all values are given in GPa

Sample	ULN1W	ULUN3W	ULUN5W
1	76.6	99.9	92.4
2	71.4	90.0	83.3
3	76.4	97.1	86.2
4	75.9	89.2	91.0
Mean	75.1	94.1	88.2
Mean and standard deviation	85.7 ± 9.1		

The curvature can therefore be determined experimentally from surface strain measurements using:

$$\varkappa = \frac{\varepsilon_T - \varepsilon_C}{D} \tag{4}$$

where ε_T is the (top surface) tensile strain, ε_C is the (bottom surface) compressive strain and D is the diameter of the pipe.

As noted in the previous section, the experimental stress-strain data could be described by a fifth order polynomial curve, that is:

$$\sigma = A_5\varepsilon^5 + A_4\varepsilon^4 A_3\varepsilon^3 + A_2\varepsilon^2 + A_1\varepsilon + A_0 \tag{5}$$

where $A_0, \ldots A_5$ are material constants.

Combining Equations (3) and (5) gives,

$$\sigma = A_5 y^5 \varkappa^5 + A_4 y^4 \varkappa^4 + A_3 y^3 \varkappa^3 + A_2 y^2 \varkappa^2 + A_1 y\varkappa + A_0 \tag{6}$$

We now consider the geometry of the pipe section (Figure 9). The force on an element of area $(D/2)$. t . $\delta\theta$ is given by:

$$\delta F = [A_5 y^5 \varkappa^5 + A_4 y^4 \varkappa^4 + A^3 y^3 \varkappa^3 + A_2 y^2 \varkappa^2 + A_1 y\varkappa + A_0]\frac{D}{2} t\delta\theta \tag{7}$$

Noting that:

$$y = \frac{d}{2}\sin\theta \tag{8}$$

We can use Equations (7) and (8) to obtain an expression for the bending moment:

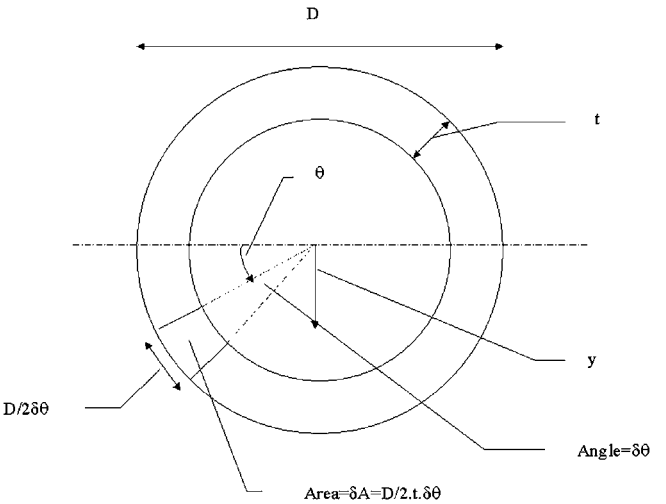

Figure 9 | Schematic representation of an element under stress.

$$M = 4\int_0^{\frac{\pi}{2}}\left[A_5\left(\frac{D}{2}\sin\theta\right)^5\varkappa^5 + A_4\left(\frac{D}{2}\sin\theta\right)^4\varkappa^4 + A_3\left(\frac{D}{2}\sin\theta\right)^3\varkappa^3 + A_2\left(\frac{D}{2}\sin\theta\right)^2\varkappa^2 + A_1\left(\frac{D}{2}\sin\theta\right)\varkappa + A_0\right]\frac{D}{2}t.\frac{D}{2}\sin\theta d\theta \quad (9)$$

which after some simplification reduces to:

$$M = D^2t\left[A_5\left(\frac{D}{2}\right)^5\varkappa^5\int_0^{\frac{\pi}{2}}\sin^6\theta d\theta + A_4\left(\frac{D}{2}\right)^4\varkappa^4\int_0^{\frac{\pi}{2}}\sin^5\theta d\theta + A_3\left(\frac{D}{2}\right)^3\varkappa^3\int_0^{\frac{\pi}{2}}\sin^4\theta d\theta + A_2\left(\frac{D}{2}\right)^2\varkappa^2\int_0^{\frac{\pi}{2}}\sin^3\theta d\theta + A_1\left(\frac{D}{2}\right)\varkappa\int_0^{\frac{\pi}{2}}\sin^2\theta d\theta + A_0\int_0^{\frac{\pi}{2}}\sin\theta d\theta\right] \quad (10)$$

Equation (10) enables the moment-curvature relationship for a pipe to be calculated using the constants from the tensile stress-strain tests.

Estimating the maximum tensile stress in the pipe at fracture

The analysis presented above enables the maximum stress in the pipe at failure to be estimated as follows. The moment-curvature relationship (Equation 10) enables the curvature at failure, $\varkappa_f$, to be determined from the bending moment at failure and the relevant material constants that characterise the tensile stress-strain response. The corresponding value of the maximum strain in the pipe follows from:

$$\varepsilon_f = \frac{D}{2}K_f \quad (11)$$

The surface stress at failure can then be found using Equation (5). This failure stress based on non-linear analysis may subsequently be compared with failure stresses determined using simple bending theory and used to derive a correction factor, as explained below.

FLEXURAL BEHAVIOUR OF THE LINED PIPES

Failure observation

Most pipes appeared to fail in tension, with pipe fracture initiating at the bottom surface of the pipe, the invert. However, some failures appeared to be due to either compression, or local buckling in the compressive region of the pipe. These failures were usually associated with very thin wall thicknesses corresponding to pipes with very asymmetric cross-sections. In some cases the pipe manufacturer had used chaplets (casting supports) in order to reduce the asymmetry of pipe wall thickness resulting from core movement during the casting process. On one occasion such a chaplet acted as a large defect and led to premature pipe failure; this result was discarded.

The two types of interactive liner remained intact during all the tests, even though the cast iron host pipes underwent catastrophic failure. Some of the developmental liner samples showed some minor perforation, but this was believed to be associated with large, post-failure, relative displacements of the broken sections of host-pipe, which are unlikely to occur in well-supported pipes buried

Table 2 | Pipe failure stresses based on linear and non-linear analysis

	ULN1W	ULUN3W	ULUN5W
Pipe stress at failure (elastic analysis) (MPa)	160	270	242
Pipe stress at failure (non-linear analysis) (MPa)	101	168	147
Ratio of values	0.63	0.62	0.61

in the ground. In pressurised tests, water pressure was maintained for a short while subsequent to host pipe failure and unperforated liners were able to withstand this condition. The ability of the liners to survive the wet tests showed that their behaviour was essentially unchanged by the presence of water and the associated pressure and increased level of liner/host-pipe surface interaction.

The observation that semi-structural liners are capable of surviving host-pipe failure is potentially a significant outcome, both in terms of industrial design procedures and also for the liner manufacturers and the water utilities.

QUANTITATIVE ANALYSIS OF TESTS

The approach described above was applied to the pipe tests for which the tensile behaviour parameters were subsequently measured, enabling the bending moments at failure to be converted to values for the maximum stress in the pipe. These stress values were then compared with those calculated based on a linear elastic analysis, so that a correction factor could be deduced, enabling all the strength data from tests analysed elastically to be modified. Table 2 shows the results for the three pipes for which both tensile test and bend test data were available (ULN1W, ULUN3W and ULUN5W).

Based on Table 2, the ratio of the failure stress determined using non-linear arguments, to that obtained using linear elastic assumptions is taken as 0.62. This correction factor was applied to the data based on elastic analysis reported previously. Figure 10 shows all of the data for the full range of pipes tested.

Examination of the data indicates that at any given condition there is some spread. This is believed to be due to material variability, for un-notched samples, and material variability combined with variations in notch geometry, for notched samples. The notched samples show a lower strength, as expected. There is no obvious variation in the results for the dry tests and the corresponding wet tests. Hence in Table 3 (where the results from different liners can be compared), dry and wet data are averaged together. It is clear from Table 3 that there is no clear effect of liner type on the pipe failure strength. Figure 11 shows this graphically. The apparent variations in pipe strengths in the plot are thought to be due to material variability, batch to batch variation differences in processing and so on.

It is also useful if a value for the modulus of the material can be obtained from bending results to enable a comparison with the moduli obtained from the tensile tests and hence provide greater confidence in the results obtained. The bending moment-curvature plot, Figure 12, has a slope EI. Thus by taking the slope of the curve using curve fitting procedures and then dividing the value obtained by the second moment of area, I, for the pipe concerned, an approximate value for the modulus of the pipe at zero curvature may be obtained.

It can be seen from Table 4 that there is reasonable agreement between the four values of modulus obtained; the mean value is 111 GPa, which is in the accepted range of moduli for cast iron (Angus 1976).

Applying the non-linear approach

Figure 13 shows the experimental stress-strain data for specimen ULN1W and the associated regression curve. The R^2 value determined indicates that the numerical fit is excellent within the range of values represented by the experimental data. The equation of the regression line, at the bottom of the plot, enables values for the required A-type coefficients to be found.

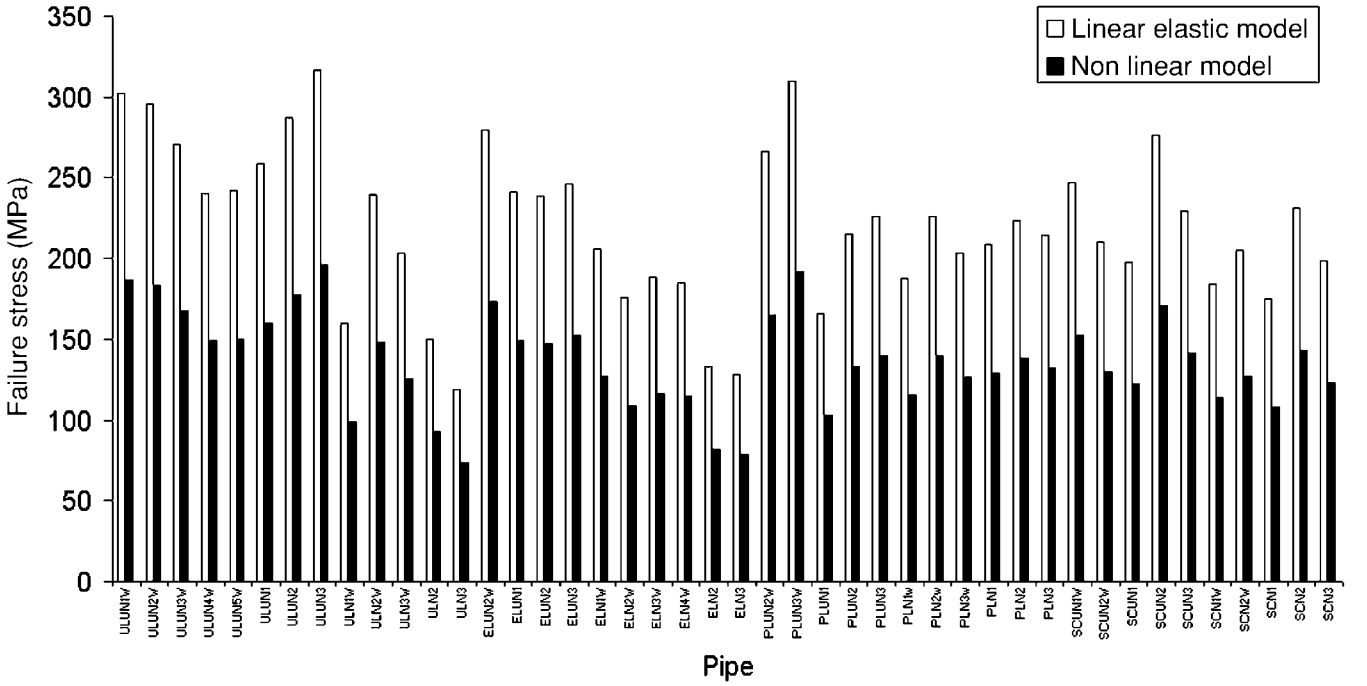

Figure 10 | Bar chart of the failure strengths for all pipes, showing values obtained using both the linear elastic approach and the non-linear analysis.

Table 3 | Table showing the mean gross failure stress and standard deviation for all samples tested, using the non-linear model

Sample type	Mean gross failure stress (MPa)	Standard deviation (±MPa)
Unlined, un-notched	171	16
Epoxy lined, un-notched	156	10
New development, un-notched	146	30
Sub-coil, un-notched	144	17
Unlined, notched	108	26
Epoxy lined, notched	105	18
New development, notched	130	8
Sub-coil, notched	123	12

Table 4 | Table showing slope, the second moment of area, I, and elastic modulus for the pipes in bending, E

Specimen	I (m^4)	E (GPa)
SCUN2	6.92E-06	107
ULUN2	9.23E-06	108
ULN4	7.50E-06	120
ULN5	6.56E-06	109

The non-linear approach developed above was used to derive predicted bending moment-curvature plots for two pipes. The actual bending moment-curvature plot, derived as described above, was then compared against these predicted plots. Each plot shows 13 curves, one is the actual bending moment-curvature response, whilst the other 12 are those predicted using data for the coefficients obtained from the 12 tensile tests (four repeats from three samples).

Figure 14 shows the predicted and measured bending moment-curvature response for an un-notched pipe. It can be seen that the predicted data are reasonably accurate at low values of curvature. However at high curvatures the predicted values can deviate markedly from

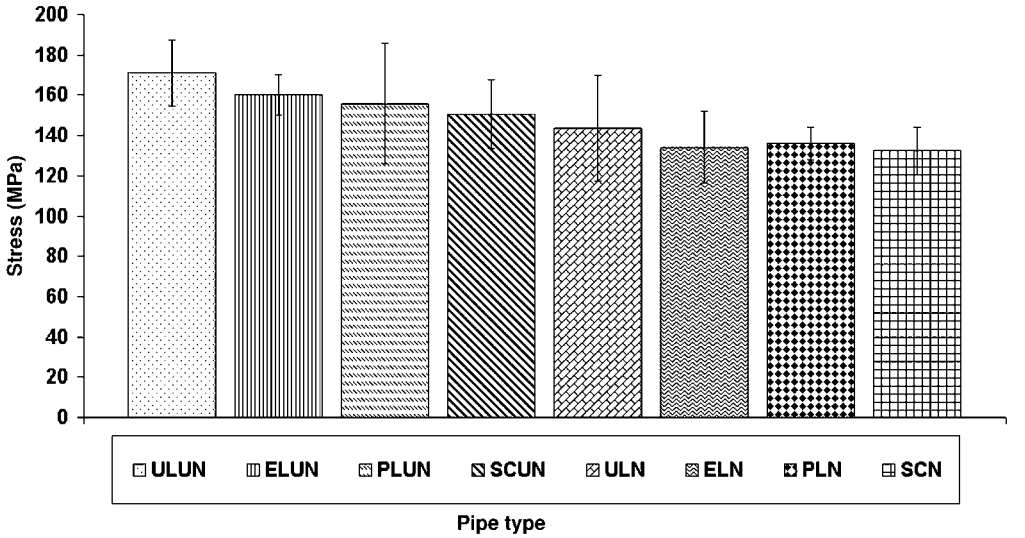

Figure 11 | Plot showing the variation of mean gross failure stress and standard deviation for all samples.

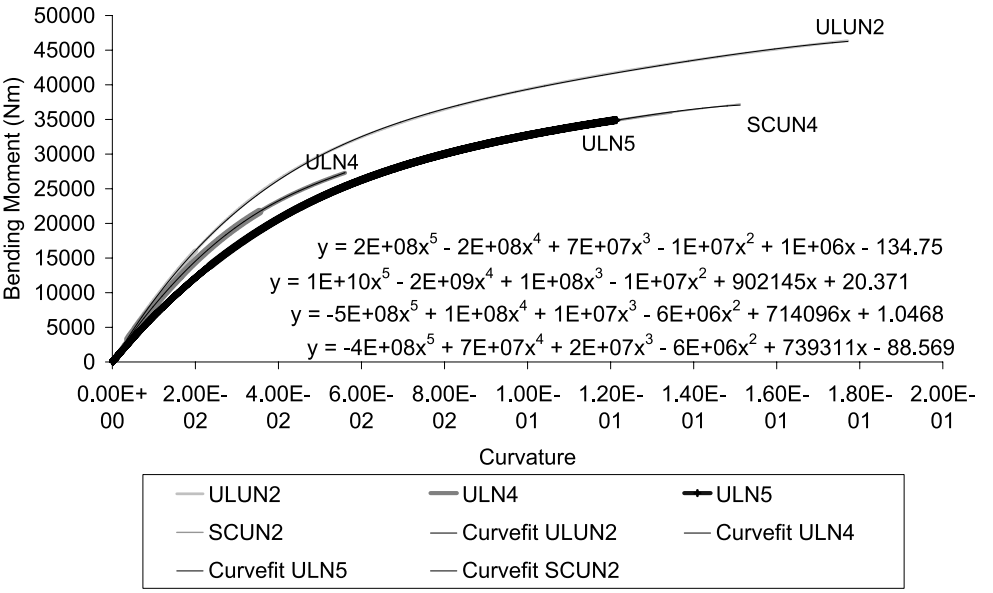

Figure 12 | Plot of bending moment versus curvature for the pipes in bending; the curve fits are also given, with the equations for the line.

the measured data. There are two causes for this deviation. The first is that, at lower curvatures, there is less magnification of any errors in the model. The second is that the polynomial curve fit, used to obtain the values of the coefficients used in the model, are only accurate within the range of data represented by that particular

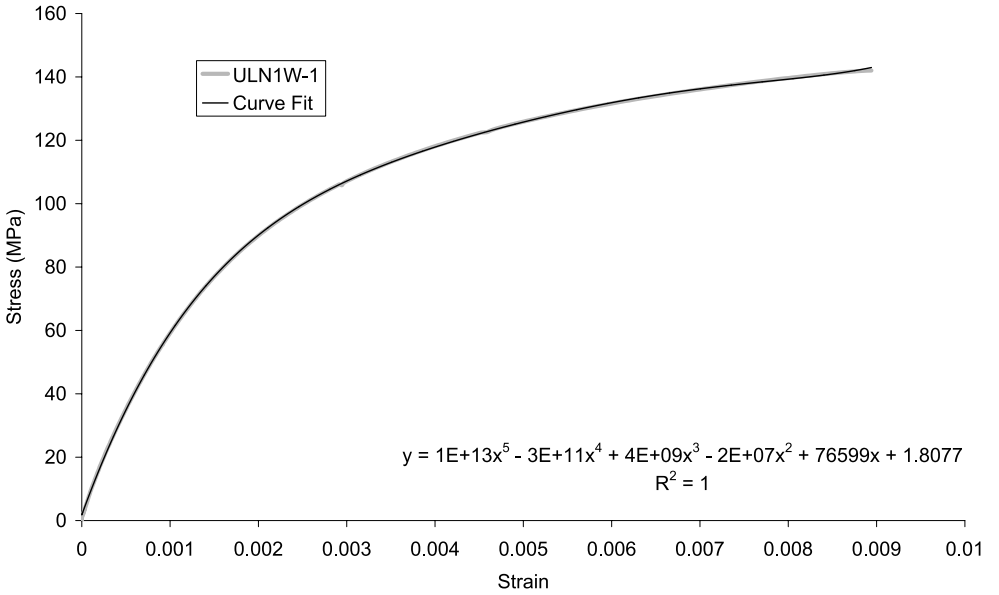

Figure 13 | Experimental stress-strain data (faint line) for specimen ULN1W and the associated regression curve (thin black line).

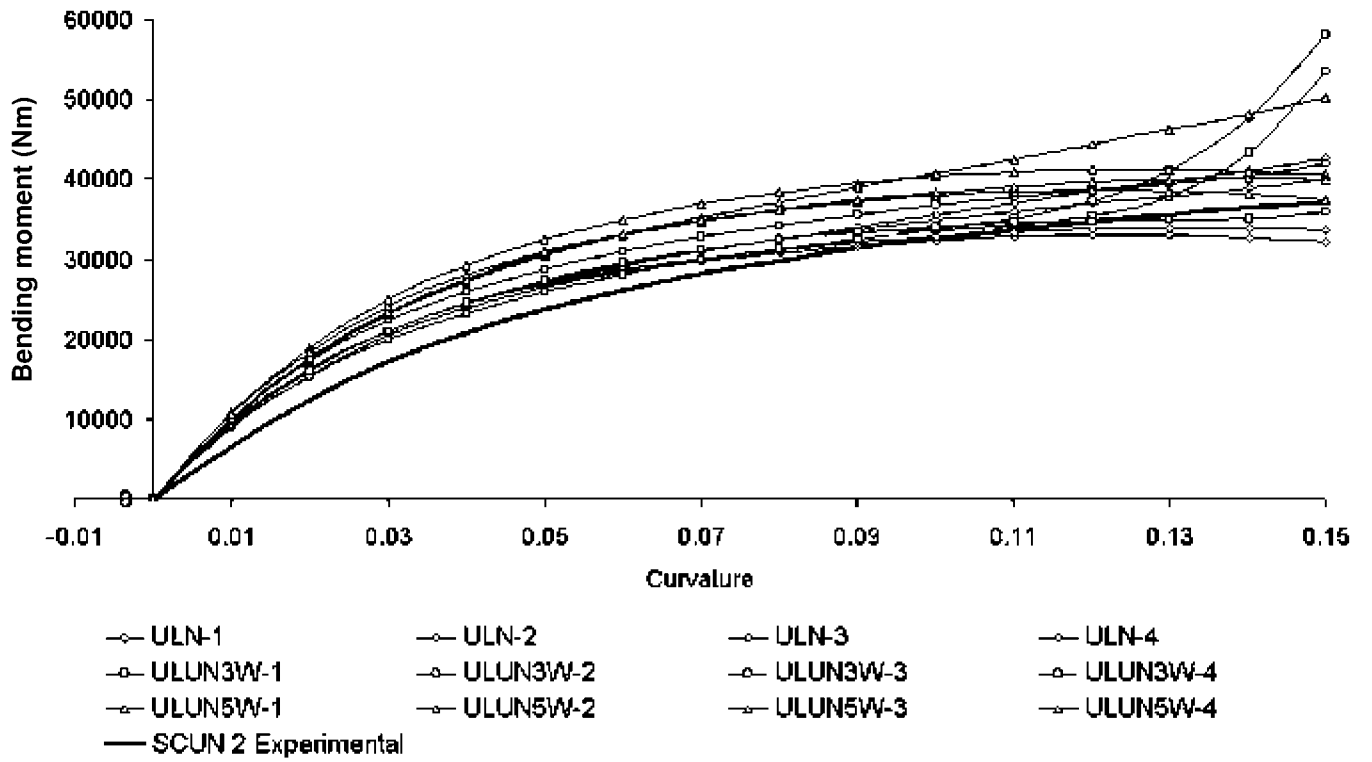

Figure 14 | Plot of predicted and experimental bending moment versus curvature for specimen SCUN2.

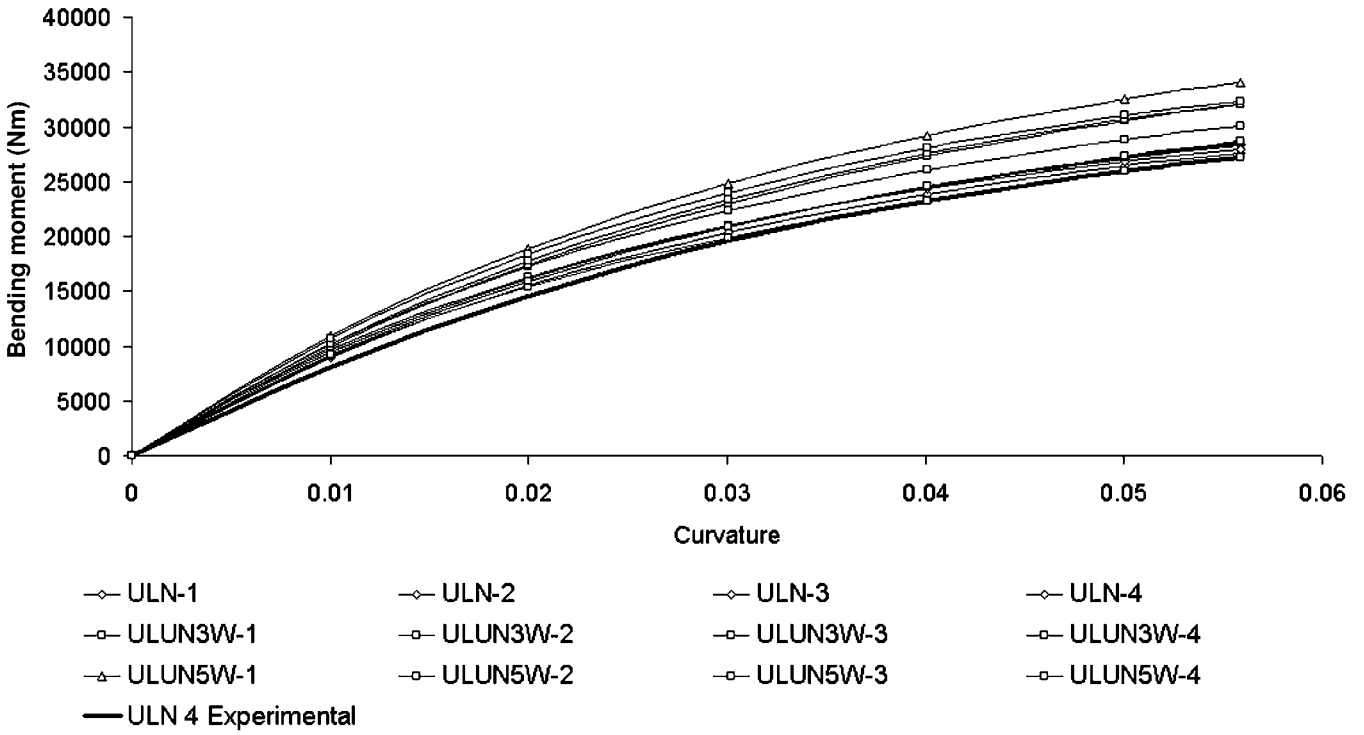

Figure 15 | Plot of predicted and experimental bending moment versus curvature for ULN4.

stress-strain plot. Therefore at elevated curvatures, corresponding to greater strains, the range over which the calculated coefficients are accurate is exceeded and so large deviations can occur.

These large deviations are not seen in the case of the notched samples, since the presence of the notch prevents the specimens from reaching the elevated curvatures possible in the un-notched pipes. Figure 15 shows the predicted and measured bending moment-curvature response for a notched sample. Less deviation from the measured values is seen in comparison with the un-notched specimens.

Comparing tensile and bend test results

An obvious comparison that can be drawn between the tensile and bend test data is in the measured elastic moduli. The tensile test data gave a mean elastic modulus of 85.7 GPa, whereas the mean elastic modulus in bending was 111 GPa. This disagreement may be explained by considering the stress arrangement within the test arrangements, and the inherent non-linearity of the material.

In the tensile tests the stress level is constant across the section. This means that, even though the material is non-linear, the sample behaves as if it is equally 'stiff' across the section, that is, any reduction in elastic modulus with increasing stress is uniformly experienced across the section. However, in the bending specimens the stress varies across the section, since the stress level is dependent upon the distance from the neutral axis, as well as varying between tension and compression. This means that, for any given stress in the outer circumference of the pipe, the stress at the inner circumference will be less. Since the stress at the inner circumference is less, the material in that region is effectively stiffer, because of the non-linearity of the material. The overall effect is to make samples in bending appear stiffer than those in tension at any given stress value.

The other way in which tensile and bending results may be compared is using the bending moment-curvature plot (Figures 14 and 15). This may be directly derived from the tests on whole pipes or obtained from tensile test data, as described above. The agreement between the two sets of data, given the degree of non-linearity of the material is fair, particularly at low curvatures. However, at higher values of curvature, the agreement becomes less accurate owing to the factors mentioned in the previous section.

CONCLUDING REMARKS

The behaviour of lined cast-iron pipes has been investigated. Metallography revealed the material to be a typical grey cast iron, with a pearlitic matrix along with graphite flakes of assorted morphology. Tensile tests carried out on the material revealed it to be highly non-linear, which is not unusual for a grey cast iron. The tensile tests were also used to determine a value for the modulus of the material, by considering the modulus at zero strain. The modulus as determined from the tensile data was around 86 GPa. Four-point bending tests to failure were also carried out on pipes lined with three different liners, an unlined control was also considered.

The bending moment-curvature response of the material was determined. This was used to determine the modulus of the material. Bending moment-curvature data suggested that the modulus of the material was around 111 GPa. This apparent discrepancy in the modulus values in tension and bending can be accounted for by considering the stress system in the two different cases relative to the non-linearity of the material. In order to enable comparison between tensile and bending data a non-linear analysis has been developed that allows tensile data to be used to derive the material response in bending. Data derived using this model were found to be in reasonable agreement with measured data within the range of curvatures experienced during the testing programme.

With regard to the performance of the liners, when lined cast iron pipes were tested to failure in four-point bending, interactive liners survived host-pipe failure, whilst, as expected, the non-structural liner did not. Further work is needed to investigate the behaviour of interactive liners under conditions that occur following host-pipe fracture. In particular long-term performance data are also required and in this context it may be relevant to consider the ageing of the polyethylene and resistance to chemical and other forms of attack, whilst under load.

REFERENCES

Angus, H. T. 1976 *Cast Iron: Physical and Engineering Properties*. Butterworths, London.

Boot, J. C. & Toropova, I. L. 1999 Polyethylene thin-walled liners for water mains: development of structural design guidelines. *Trenchless Technology Research* **14**(2), 13–28.

Boot, J. C. & Welch, A. J. 1996 Creep buckling of thin-walled polymeric pipe linings subject to external groundwater pressure. *Thin Walled Structures* **24**, 191–210.

Boot, J. C., Guan, Z. W. & Toropova, I. 1996 The structural performance of thin-walled polyethylene pipe linings for the renovation of water mains. *Trenchless Technology Research* **11**(1), 37–51.

Crunkhorn, B. B., Smith, P. A., Mulheron, M. & Whiter, J. T. 2001 Examining the performance of semi-structural pipe liners. *Proceedings of Plastics Pipes XI Conference, September 2001*. Institute of Materials, Munich, Germany.

Gumbel, J. E. 1997 Structural design of pipe linings: review of principles, practice and current developments around the world. *Proceedings of International No Dig '97*, Taipei.

UKWIR (1999) Pipeline innovation and plastics pipe systems. *Proceedings of the 5th Annual UKWIR Research Dissemination Seminar*, 13th April 1999, University of Warwick, UK.

First received 31 July 2003; accepted in revised form 5 May 2004